

Chiral and Isotope Analyses for Assessing the Degradation of Organic Contaminants in the Environment: Rayleigh Dependence

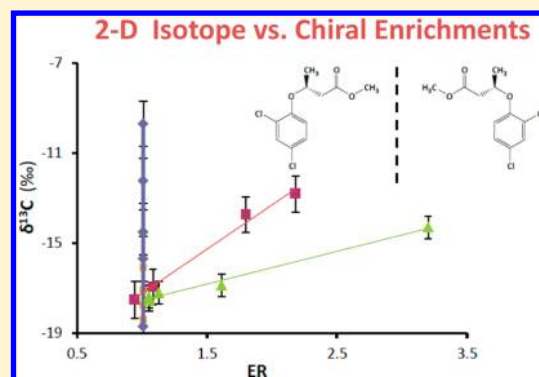
S. Jammer,[†] A. Voloshenko,[†] F. Gelman,^{*,‡} and O. Lev^{*,†}

[†]The Casali Center of Applied Chemistry, The Institute of Chemistry, The Hebrew University of Jerusalem, Jerusalem 91904, Israel

[‡]The Geological Survey of Israel, Jerusalem 95501, Israel

Supporting Information

ABSTRACT: The Rayleigh equation is frequently used to describe isotope fractionation as a function of conversion. In this article we propose to draw a parallel between isotope and enantiomeric enrichments and derive a set of conditions that allow the use of the Rayleigh approach to describe the enantiomeric enrichment–conversion dependencies. We demonstrate an implementation of the Rayleigh equation for the enantioselective enzymatic hydrolysis of Mecoprop-methyl, Dichlorprop-methyl, and dimethyl-methylsuccinate by lipases from *Pseudomonas fluorescens*, *Pseudomonas cepacia*, and *Candida rugosa*. The data obtained for all the studied reactions gave good fits to the Rayleigh equation, with a linear regression $R^2 > 0.96$. In addition to that, our analysis of four microcosm studies on the hydrolysis of the individual enantiomers of Dichlorprop methyl, Lactofen, Fenoxaprop-ethyl, and Metalaxyl reported in the literature by other research groups revealed a suitability of the Rayleigh dependence. Two dimensional plots describing the isotope fractionation versus enantiomeric enrichment are demonstrated for all studied cases. Processes not accompanied by enantiomeric enrichment (acid and base hydrolysis) and by isotope enrichment (transesterification) are demonstrated, their 2-D plots are either horizontal or vertical which can illuminate concealed degradation pathways.



INTRODUCTION

The concept of stable isotope fractionation relies on the observation of shifts in ratios of stable isotopes caused by the breakage or generation of chemical bonds during chemical transformations. During recent decades compound specific isotope analysis (CSIA) has undergone a rapid development toward important applications in contaminant hydrology and organic biogeochemistry providing evidence of pollutant degradation within contaminant aquifers.^{1–3} Multielemental CSIA has been shown to be applicable for the determination of degradation pathways of many organic contaminants, including pesticides.^{4–19}

Increasing scientific attention to organic micropollutants and their occurrence in environmental systems brought growing research attention to micropollutant stereoisomers, probing the toxicity and metabolic pathways that may largely depend on chirality. Comprehensive literature and several reviews on stereoisomeric selectivity and enantiomeric enrichment of micropollutants in effluents and contaminated streams have appeared in recent years.^{20–22}

The observed enantiomeric enrichment of organic micropollutants, expressed as the ratio between the enantiomers (ER) can be used as a tracer tool in environmental studies.²³ It has been demonstrated that shifts in the ER can be used for source tracking²⁴ and elucidation of degradation pathways.^{25,26} Enantioselective degradation of chiral pesticides in polluted aquifers have been studied recently. Zipper et al.²⁷ used chiral

analysis to detect in situ microbial biotransformation of Mecoprop that has leached to contaminated aquifers. Monkiedje et al.²⁸ reported on different enantiomeric enrichment rates of Metalaxyl in landfill soils indicating on site-specific differences in microbial populations responsible for the pesticide transformation.

In this article we focused on the enantioselective hydrolysis of esters by different types of lipase. Lipase is an important class of the hydrolytic enzymes²⁹ excreted to the environment by plant roots and microorganisms, showing a wide specificity to high regio- and enantioselective hydrolytic reactions.^{30,31} Many pollutants such as organophosphorus pesticides, synthetic polyesters, and polyamides are reported to be degraded by lipase.^{32,33}

The parallel process of comparing the enrichment of one species relative to the other is applied in both CSIA and enantiomeric analysis to prove existence of biodegradation. Recently, Badea et al.³⁴ presented a first example of enantioselective isotope analysis (ESIA) applied to the insecticide α -hexachlorocyclohexane, and Maier et al.³⁵ used ESIA to demonstrate the enantioselective biodegradation of three polar herbicides. In a previous work of our research

Received: September 11, 2013

Revised: January 26, 2014

Accepted: January 28, 2014

Published: January 28, 2014

group³⁶ we suggested that enantiomeric enrichment can be used for source tracking and for discrimination between domestic and nondomestic wastewater pollution and have demonstrated that the Rayleigh approach can fit the enantiomeric enrichment of venlafaxine in a microcosms study.

The mathematical description of the relation between the extent of degradation and isotopic composition of the investigated compound can be expressed by the Rayleigh equation (eq 1):

$$\frac{R_t}{R_0} = f^\epsilon \quad (1)$$

R_t and R_0 represent the initial and conversion-dependent isotope ratio, f is the residual fraction (C_t/C_0), and ϵ represents the isotope enrichment factor.

The isotope enrichment factor, ϵ , usually expressed in per mill units (‰) can be obtained as a slope of the linear regression line of natural logarithm of the isotopic enrichment, R_t/R_0 , against the natural logarithm of the extent of degradation (eq 2).

$$\ln \frac{R_t}{R_0} = \epsilon \times \ln f \quad (2)$$

In this article we aim to support the concept of applying the Rayleigh approximation to enantioselective processes. We suggest that the Rayleigh equation can be expressed in the same way for enantiomeric fractionation, replacing R_t and R_0 with the enantiomeric enrichment ER_t and ER_0 , and using the enantiomeric enrichment factor ϵ_{ER} expressed in percent (eq 3).

$$\ln \frac{ER_t}{ER_0} = \epsilon_{ER} \times \ln f \quad (3)$$

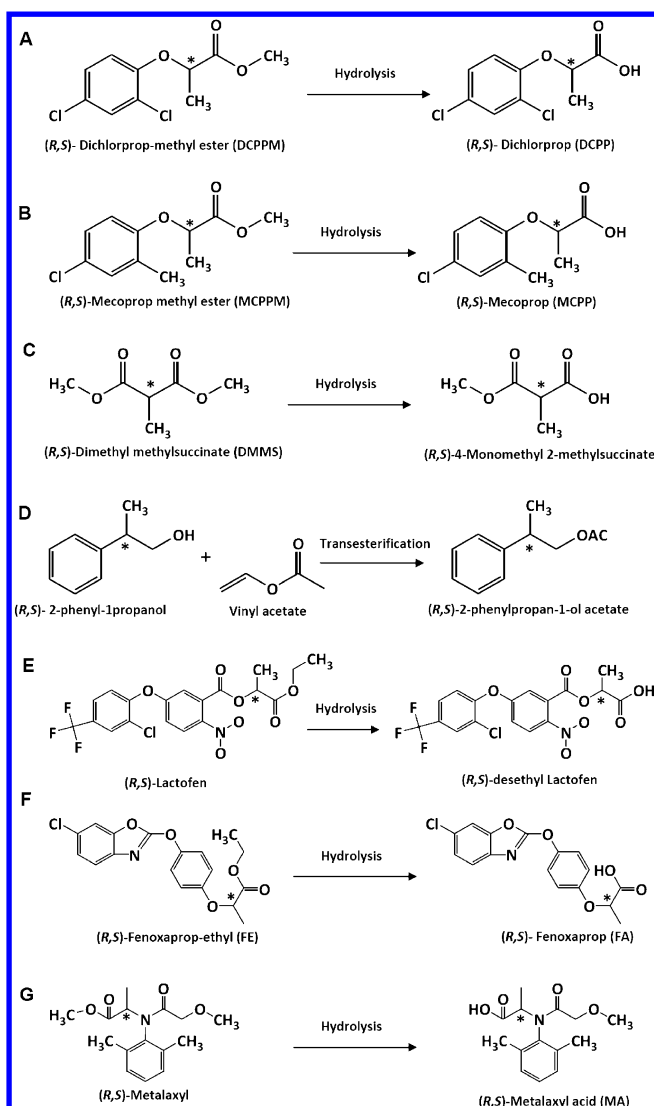
In this paper we define ER as a ratio between the more abundant to the less abundant enantiomer, then in all cases $ER > 1$.

We choose to exemplify our idea on phenoxyalkanoic methyl herbicides (Scheme 1A,B): (*R,S*)-Mecoprop-methyl (methyl-2-(4-chloro-2-methylphenoxy)propanoate) and (*R,S*) Dichlorprop-methyl (methyl-2-(2,4-dichlorophenoxy)propionate), ubiquitous water contaminants.³⁷ We consider also extreme cases: no enantiomeric enrichment by the chemical conversion of (*R,S*)-dimethyl-2-methylsuccinate DMMS (Scheme 1C) and no isotope enrichment in the enzyme catalyzed transesterification of the chiral alcohol (*R,S*)-2-phenyl-1-propanol (Scheme 1D). In addition to the above, four recently published reports describing the kinetics of the hydrolysis of individual enantiomers of (*R,S*)-Dichlorprop methyl,³⁸ (*R,S*)-Lactofen (1-ethoxy-1-oxo-2-propanyl-5-[2-chloro-4-(trifluoromethyl)phenoxy]2-nitrobenzoate),³⁹ (*R,S*)-Fenoxaprop-ethyl (ethyl-2-(4-(6-chloro-2-benzoxazolyloxy)phenoxy)propionate)⁴⁰ and (*R,S*)-Metalaxyl (methyl N-(2,6-dimethylphenyl)-N-(methoxyacetyl)alaninate),²⁸ in microcosm studies are analyzed and their Rayleigh dependency is reconstructed. The conditions for obtaining a good Rayleigh fit are derived and we examine to what extent those are met in the study-cases presented in this article.

EXPERIMENTAL SECTION

Materials and Methods. Materials and reagents are described in the Supporting Information (SI).

Scheme 1. Chemical Structures and Transformations of the Chiral Substrates Discussed in This Article^a



^aChiral center is denoted by an asterisk (*).

All the studied reactions were carried out at 21 ± 2 °C, under constant mixing. The kinetic tracking of the transformations was carried out in parallel separate vials and the whole content of each vial was used for a single analysis. Detailed reaction and extraction procedures can be found in the SI.

Analytical Methods. Enantiomeric Enrichment Analysis. The chiral reactants (*R,S*)-DCPPM, (*R,S*)-DMMS, (*R,S*)-MCPPM and the hydrolysis products DCPP and MCPP were analyzed by GC-SMB-QQQ-MS (a combined instrument comprised of GC, Agilent 7890A, Aviv Analytical supermolecular beam ion source⁴¹ and Agilent 7000A triple quadrupole mass spectrometer), equipped with a chiral column (β -cyclodextrin, 1310Srt-bDEXsm, 30 m \times 250 μ m \times 0.25 μ m; Restek). Detailed analytical method is presented in the SI. The DMMS hydrolysis product, 4-monomethyl 2-methylsuccinic acid, was determined by preparative HPLC, followed by methylation and analyzed by GC-MS (detailed in the SI).

Isotope Analysis. Carbon isotope analysis of all the reactants was carried out with a gas chromatograph-combustion-isotope ratio mass spectrometer (GC-C-IRMS)

(Trace GC ultra-Delta V Plus IRMS; Thermo Scientific). Detailed analytical method is presented in the SI.

RESULTS

Analysis of the Degradation of Phenoxyalkanoic Methyl Herbicides. The kinetic tracking of (*R,S*)-DCPPM and (*R,S*)-MCPPM in the enzymatic degradation (pH 7.4) gave a first order kinetic fit (Figure 1A) with overall rate constants in

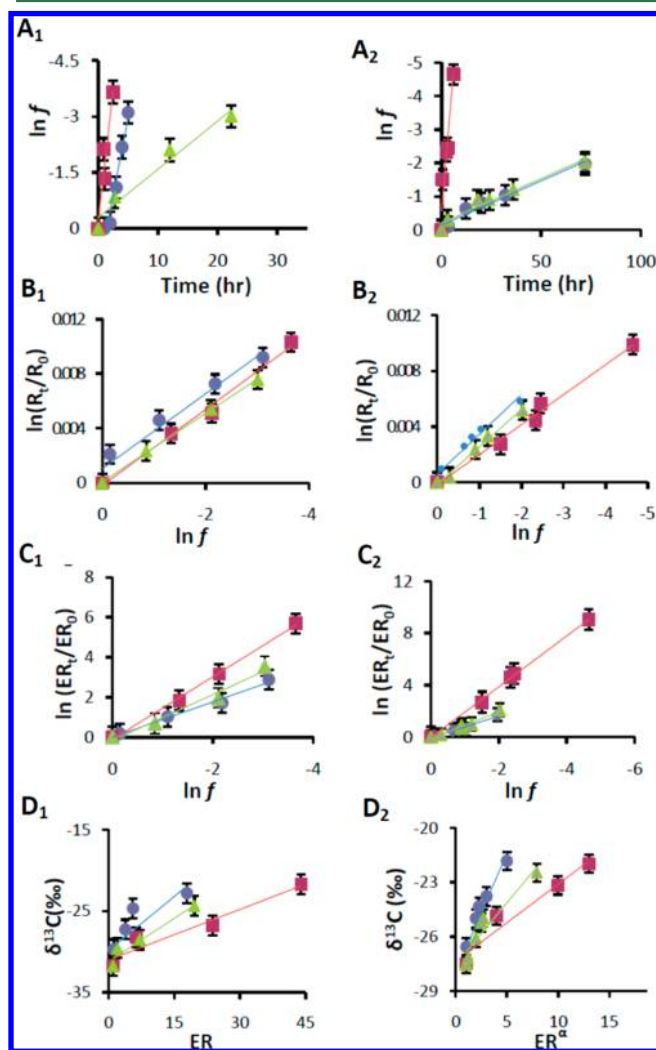


Figure 1. Enzymatic hydrolysis of DCPPM (1) and MCPPM (2). (A₁, A₂) first order kinetic fit; (B₁, B₂) Isotope enrichment (Rayleigh fit); (C₁, C₂) Enantiomeric enrichment (Rayleigh-like-fit); (D₁, D₂) Isotope fractionation vs enantiomeric enrichment. α The point ER = 8480; $\delta^{13}\text{C} = -17.8$ for *Candida rugosa* was omitted to keep a realistic scale. (green triangle) Lipase from *Pseudomonas fluorescens*; (red square) Lipase from *Candida rugosa*; (blue circle) Lipase from *Pseudomonas cepacia*.

the range of 0.036–1.002 h⁻¹ and correlation coefficients in the range of 0.93–0.96 for the various enzymatic reactions (detailed in SI Table S1). The isotope fractionation followed the Rayleigh dependence, $R^2 = 0.96$ –0.99 (Figure 1B), and the linear fit to the Rayleigh approximation was also obtained for enantiomeric enrichment, $R^2 = 0.96$ –0.99 (Figure 1C) obtaining the enantiomeric and isotope enrichment factors detailed in Table 1. The two-dimensional plots (Figure 1D) describing the isotope fractionation versus enantiomeric

enrichment showed a linear correlation, with correlation coefficients of 0.92–0.99. The slopes for these linear regressions are detailed in Table S2 in the SI.

Enzymatic and Chemical Hydrolysis of (*R,S*)-DMMS.

The acid and alkaline hydrolysis reactions of (*R,S*)-DMMS followed first order kinetics (Figure 2A₂) with degradation rate constants of 0.016 h⁻¹ and 0.52 h⁻¹, respectively, ($R^2 = 0.96$). As expected, during these reactions chirality was unaffected by the conversion and only the isotope composition has changed with very similar isotope enrichment factors of $\pm 2\%$ as in Table 1 (Figure 2B₂, 2C₂). In the enzymatic hydrolysis, DMMS was enriched isotopically and enantiomerically following first order kinetics (Figure 2A₁, Table S1 in the SI) and Rayleigh dependence in both cases, with correlation coefficients in the range of 0.94–0.99 (Figure 2B₁, C₁, Table 1). The two-dimensional plot (Figure 2D) describing the isotope fractionation versus the enantiomeric enrichments can provide a powerful visual distinction between the biotic and abiotic reactions via chiral analysis, as only the chemical processes are described by vertical lines.

Enzyme-Catalyzed Eneantioselective Transesterification Reaction. The kinetics of the transesterification reaction fit the first order rate law with $k = 0.135$ h⁻¹ ($R^2 = 0.97$) (Figure 3A), CSIA showed no isotope enrichment and the enantiomeric enrichment followed the Rayleigh dependence with a correlation coefficient of 0.98, giving the enantiomeric enrichment factor of $-213.1 \pm 7.2\%$ (Figure 3B–D).

Reconstruction of Rayleigh Dependence Based on Reported Microcosm Studies. In addition to the enzymatic hydrolytic reactions, we decided to verify a compatibility of the Rayleigh approximation to reported microcosm studies; we focused on studies published in the literature describing the kinetics of the hydrolysis of individual enantiomers of pesticides as Dichlorprop methyl, as in our enzymatic research, and others.

We choose four studies which were carried out with field soils or sediments under near neutral pH conditions.

Ma et al.³⁸ reported on the enantiomeric degradation of Dichlorprop methyl (Scheme 1A) by a bacterial strain identified as *Pseudomonas sp.*, isolated from an activated sludge from the aerobic tank of a textile-printing wastewater treatment plant. The authors compared the enantioselective biodegradation at different pH solutions (pH: 5, 7, 9). The authors provided the first order degradation rate constants as 0.124, 0.119, and 0.055 h⁻¹ for pH 5, 7, and 9, respectively, with $R^2 = 0.98$, 0.97, and 0.96, respectively. Reconstruction of the Rayleigh dependence, based on the data provided in Figure 7 in ref 38 and the first order rate constants said above, obtained the enantiomeric enrichment factors of 22.1 ± 5.5 , 44.6 ± 3.7 , and $86.9 \pm 16.5\%$ for pH 5, 7, and 9, respectively, with a correlation coefficient of 0.98 (Figure 4A).

Diao et al.³⁹ reported on the chiral hydrolysis of Lactofen (Scheme 1E), a nitrophenyl ether selective herbicide that has low water solubility and a high binding potential to soil. The enantioselectivity of Lactofen and its chiral metabolite during their biodegradation in Liao-River sediment were evaluated by laboratory sediment incubation experiments at pH 7.2. Based on the data in Figure 3a in ref 39 providing the concentration of each enantiomer during the time of the degradation experiment, we have calculated the overall first order kinetic constant to be 0.448 day⁻¹, $R^2 = 0.97$ (Figure 4C); and the authors provided the individual degradation constants for S-(+)-Lactofen and R(-)-Lactofen to be 0.627 and 0.314 day⁻¹,

Table 1. Enantiomeric and Isotope Enrichment Factors of MCPPM, DCPM and DMMS degraded by different lipases and by chemical hydrolysis^a

hydrolysis agent/target compound	MCPPM	DCPPM	DMMS
isotope enrichment factors ϵ (‰)			
<i>Lipase from Pseudomonas fluorescens</i>	-1.9 ± 0.4 (0.98)	-2.8 ± 0.1 (0.99)	-0.8 ± 0.1 (0.99)
<i>Lipase from Candida rugosa</i>	-2.2 ± 0.5 (0.99)	-2.8 ± 0.5 (0.99)	-3.4 ± 0.5 (0.97)
<i>Lipase from Pseudomonas cepacia</i>	-2.2 ± 0.4 (0.96)	-2.7 ± 0.2 (0.96)	-0.4 ± 0.1 (0.94)
HCl	nd	nd	-2.1 ± 0.2 (0.99)
NaOH	nd	nd	-3.1 ± 0.7 (0.96)
enantiomeric enrichment factors ϵ_{ER} (%)			
<i>Lipase from Pseudomonas cepacia</i>	-46.0 ± 24.2 (0.96)	-88.6 ± 15.1 (0.98)	-64.0 ± 9.08 (0.94)
<i>Lipase from Candida gosrua</i>	-194.1 ± 4.4 (0.99)	-168.1 ± 14.1 (0.99)	-66.8 ± 12.05 (0.97)
<i>Lipase from Pseudomonas fluorescens</i>	-66.0 ± 9.6 (0.98)	-112.9 ± 21.2 (0.99)	-25.9 ± 8.5 (0.97)

^aThe regression correlation coefficient, R^2 is given in brackets; the 95% confidence interval of the slope of the regression line in the Rayleigh plots is given after the \pm sign. The enzymatic hydrolysis reactions were carried at pH 7.4, the acid hydrolysis at pH 2.1 and the alkaline hydrolysis at pH 11.5.

respectively. Based on the same data as above we were able to reconstruct the Rayleigh dependence with $\epsilon_{ER} = -42.6 \pm 4.5\%$ ($R^2 = 0.95$) (Figure 4B).

Zhang et al.⁴⁰ reported on the enantioselective environmental behavior of the chiral herbicide Fenoxaprop-ethyl. We chose to analyze the hydrolysis experiment (Scheme 1F) done with the Jiangxi Nanchang soil due to the high enantioselective degradation reported. The racemate and enantiopure S(-)- and R(+)-Fenoxaprop-ethyl were incubated with the soil suspension under nonsterilized conditions at pH 5. Based on the data in Figure 3a in ref 40, describing the degradation of the racemate we were able to calculate the overall first order degradation rate constant to be 3.86 day^{-1} ($R^2 = 0.9$) (Figure 4E), and we were able to reconstruct the Rayleigh dependence receiving an enantiomeric enrichment factor of $-23.4 \pm 4\%$ with the correlation coefficient of 0.96 (Figure 4D).

Monkiedje et al.²⁸ studied the enantioselective demethylation of unformulated racemic Metalaxyl (Scheme 1G), a phenylamide fungicide that has a tendency to migrate to deeper soil horizons with a potential to contaminate groundwater, particularly in soils with low organic matter and clay content. The authors reported the degradation rate constants as well as the correlation coefficient values for the biodegradation of unformulated racemic Metalaxyl in Cameroonian Soil and in German soil to be 0.019 day^{-1} , $R^2 = 0.97$ and 0.039 day^{-1} , $R^2 = 0.98$, respectively. Based on the concentrations of unformulated racemic Metalaxyl and its enantiomers in Cameroonian soil and in German soil after respective incubation intervals, detailed in Tables 3 and 4 in ref 28, we were able to reconstruct the Rayleigh dependence presenting the enantiomeric enrichment factors of $-85.9 \pm 6.9\%$ ($R^2 = 0.99$) and $-139.5 \pm 8.9\%$ ($R^2 = 0.97$) respectively (Figure 4F).

DISCUSSION

Analogy and Differences between Isotope and Enantiomeric Enrichments. At first glance, it seems that there is some analogy between the isotope tool and the enantiomeric one for biodegradation assessment.³⁶ However, a closer examination of the two methods leads to several

significant points of difference (Table S3 in the SI). The physical properties of isotopomers are not identical, their mass difference results in different bond energies, they tend to occupy different molar volumes and thus tend to overcome physical processes by different rates,⁴² while optical isomers have exactly the same physical properties and also the same chemical properties. This intrinsic point of difference stems from the basic factors leading to the enrichment of enantiomers and isotopomers: the enantiomers, that have the same bond strength and mass, are enriched based on the geometrical recognition and the propensity to form the diastereomers by themselves (for molecules with multiple chiral centers) or by conjugation with other chiral entities.⁴³ In contrast, isotope fractionation depends on the mass difference and the bond strength between the atoms, whereas molecular recognition is almost identical for the different isotopomers. Another significant difference is expressed in a multielemental CSIA approach in which dual isotope plots can show different transformation pathways. Chiral analysis is usually operated on molecules that have only one chiral center, but it can be used in combination with CSIA to form two-dimensional plots and to obtain further conclusions: similarity between mechanisms of degradation of two different chiral contaminants can be assessed by the similarity in the slope, when R^2 is a quality control parameter. In addition, it is noteworthy that carbon CSIA has a general limitation to be suitable mostly for relatively small ($<C_{12}$) organic molecules, due to "dilution effect"⁴² (i.e., only small fraction of the isotopes in a large molecule participate in a particularly bond cleavage). The situation can be slightly better for hydrogen due to the higher isotope fractionation factors usually obtained.⁴⁴ Thus, the ability to analyze large molecules and ease of analysis, give a degree of preference for the enantiomeric enrichment analysis. In addition, as we have seen in the case of DMMS comparing the enzymatic and chemical reactions, only the chiral tool could discriminate between those reactions,⁴⁸ whereas in the isotope analysis, close enrichment factors of $\pm 2\%$ were obtained in both cases. Moreover, in cases where there is no or very small isotope enrichment, as in the case of the transesterification said

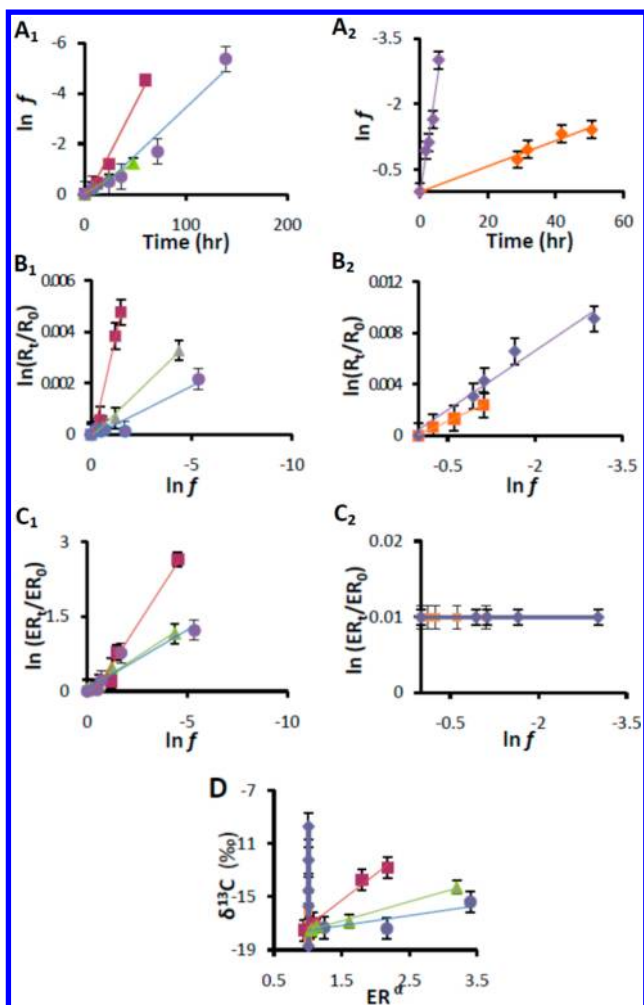


Figure 2. Enzymatic (1) and chemical (2) hydrolysis of DMMS. (A₁, A₂) First order kinetic fit; (B₁, B₂) Isotope enrichment (Rayleigh fit); (C₁, C₂) Enantiomeric enrichment (Rayleigh-like-fit); (D) Isotope fractionation vs enantiomeric enrichment. α The point $ER = 14.05$; $\delta^{13}C = -4.2$ for *Candida rugosa* was omitted in order to present a clear trend. (green triangle) Lipase from *Pseudomonas fluorescens*; (red square) Lipase from *Candida rugosa*; (blue circle) Lipase from *Pseudomonas cepacia*; (orange square) Acid hydrolysis; (purple diamond) Alkaline hydrolysis.

above, chiral analysis becomes an essential tool to teach about the biodegradation transformation. However, the main disadvantage of the chiral analysis is its restriction to the limited group of chiral molecules. Furthermore, the chiral analysis is limited to giving information regarding the conjugation and accessibility for overcoming different degradation processes. In most cases it cannot explicate the mechanistic bond cleavage pathway, unless it is measured in combination with isotope analysis.

Although chiral analysis was seldom used for source tracking as well as the Rayleigh equation for tracing the evolution of chirality, we have decided to follow the above-mentioned advantages for the enantiomer enrichment analysis, and used the Rayleigh equation to describe the enantioselective behavior in order to gain the advantages of both methods.

The use of the Rayleigh equation, originally developed for distillation of mixed liquids,⁴⁵ provides a mathematical framework for interpretation of conversion dependent isotope fractionation and is based on the assumption that molecules

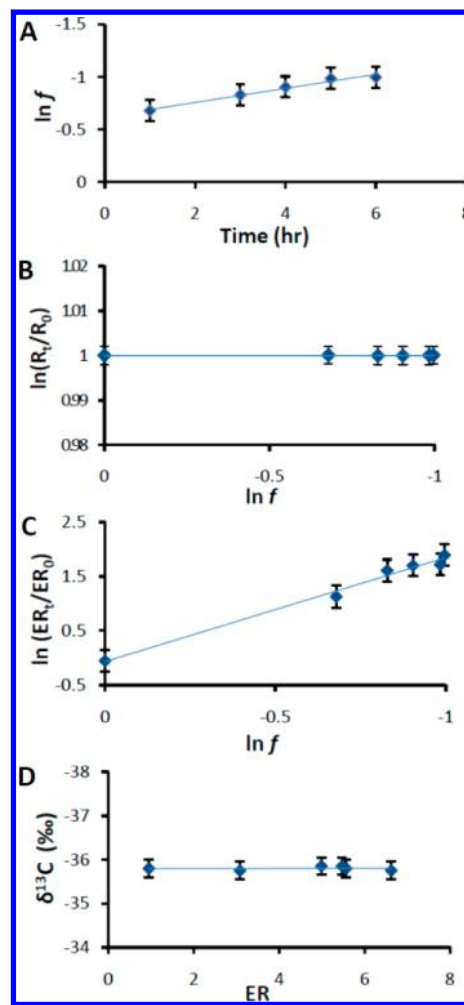


Figure 3. Transesterification of phenyl-propanol with vinyl-acetate. (A) First order kinetic fit; (B) Isotope enrichment (Rayleigh fit); (C) Enantiomeric enrichment (Rayleigh-like fit); (D) Isotope fractionation vs enantiomeric enrichment.

with light and heavy isotopes react according to first-order rate laws.⁴² However, many chemical reactions do not follow first-order kinetics, and enzymatic reactions are frequently described by the Michaelis–Menten kinetics (eq 4).

$$\frac{dC}{dt} = \frac{-kC}{[K_M + C]} \quad (4)$$

Nevertheless, in most cases the Rayleigh approximation is valid since the concentration of the heavier isotopomer is much smaller than the concentration of the lighter isotopomer. Thus, even in the case of reaction order that is larger than one, say n ($n > 1$), the rate determining step would likely involve only one molecule of the less abundant isotopes. Thus, the true reaction rate is not likely to be $-k(^L C)^n$ but rather $-k(^H C)^{n-1} (^L C)$ and thus the linear dependence of the reaction rate on the lighter isotope is obeyed.⁴² Indeed, the results we had received for the quantitative approach of using the Rayleigh equation for enantiomeric enrichments during the conversion of the chiral esters by enzymatic reactions, and the evidence we brought from microcosms studies for the suitability of the Rayleigh equation demonstrate that the use of the Rayleigh approximation for enantiomeric enrichment may be suitable for describing chiral contaminants degradation.

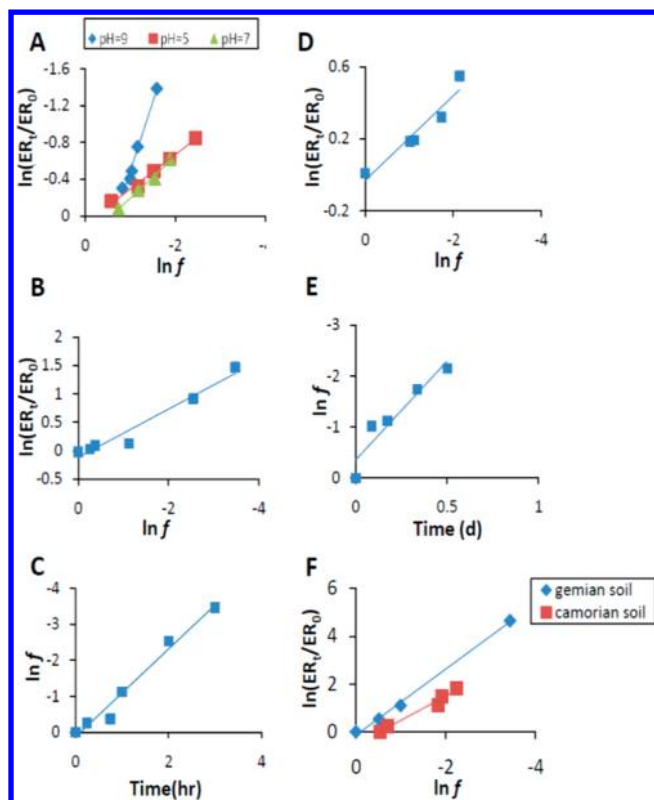


Figure 4. Lipase like activity in natural systems - microcosm studies. (A) Enantiomeric enrichment (Rayleigh-like-fit) of DCPM hydrolysis;³⁸ (B) Enantiomeric enrichment (Rayleigh-like-fit) of Lactofen hydrolysis;³⁹ (C) First order kinetic fit of Lactofen hydrolysis;³⁹ (D) Enantiomeric enrichment (Rayleigh-like fit) of FE hydrolysis;⁴⁰ (E) First order kinetic fit of FE hydrolysis;⁴⁰ (F) Enantiomeric enrichment (Rayleigh-like fit) of Metalaxyl hydrolysis.²⁸

This last conclusion left us a bit perplexed. Why did we receive Rayleigh dependency for all the examined cases, be it our controlled enzymatic tests or the four hydrolytic test cases that were described in the literature, if the Rayleigh approximation can only describe reactants under very specific conditions which do not seem relevant for environmental degradation of enantiomers? Specifically, one enantiomer is generally not much more abundant than the other and Michaelis–Menten is certainly nonlinear.

In order to conciliate this apparent problem, we consider a case where certain assumptions prevail and show the validity of the Rayleigh equation under these conditions. Later we shall verify that these conditions are rather abundant in environmental studies and hold true in the test - cases that are addressed in this paper.

Validity of the Rayleigh Approximation for Enantiomeric Enrichment. Assume a case in which the degradation rate of two enantiomers (or any other chemical entities), follow first order rate law with rate constants k_1 and k_2 , respectively. For simplicity we shall assign the concentrations of the two enantiomers by the same letters, A_1 and A_2 and assume that A_1 is less reactive, that is, $k_1 < k_2$, so we can denote $k_2 - k_1 = \bar{k} > 0$. The sum of these species $A_1 + A_2$ is denoted by C . We further assume that C is reacting at a rate that can be described by linear kinetics with an observed rate constant k_c . Under these conditions one receives (for a batch or plug flow operations) the integral equation (eq 5) and the subtracted equation (eq 6).

$$\ln \frac{A_{i,t}}{A_{i,0}} = -k_i \times t \quad (5)$$

Where A_i is A_1, A_2 or C and the subscript "0" denotes initial conditions.

$$\ln \frac{A_{1,t}/A_{2,t}}{A_{1,0}/A_{2,0}} = -(k_1 - k_2)t = \bar{k} \times t \quad (6)$$

Hence, assigning ER_t and ER_0 as A_1/A_2 at time t and at time zero, one receives eq 7

$$\ln \frac{ER_t}{ER_0} = \bar{k} \times t \quad (7)$$

Expressing t as a function of C by eq 5 and introducing it to eq 7 leads to eq 8 which is the celebrated Rayleigh equation, where the enrichment factor is given by $-(\bar{k}/k_c) = \varepsilon_{ER}$.

$$\ln \frac{ER_t}{ER_0} = -\frac{\bar{k}}{k_c} \times \ln \frac{C_t}{C_0} \quad (8)$$

Similar derivation, by expressing t as a function of $A_{1,t}/A_{1,0}$ or $A_{2,t}/A_{2,0}$ by eq 5 and introducing it to eq 7 leads to the logarithmic dependence of the enantiomeric enrichment versus the residual ($A_{i,t}/A_{i,0}$) of each enantiomer (eqs 9 and 10).

$$\ln \frac{ER_t}{ER_0} = -\frac{\bar{k}}{k_1} \times \ln \frac{A_{1,t}}{A_{1,0}} \quad (9)$$

$$\ln \frac{ER_t}{ER_0} = -\frac{\bar{k}}{k_2} \times \ln \frac{A_{2,t}}{A_{2,0}} \quad (10)$$

During the submission process of this article, Bashir et al. published an important article in this journal⁴⁶ showing that the enantioselective enrichment of hexachlorocyclohexane by *Sphingobium* spp. followed a general Rayleigh equation (eq 11)

$$\ln \frac{ER_t}{ER_0} = \varepsilon_2 \times \ln \frac{C_t}{C_0} \left[\frac{(1 + ER_0)}{(1 + ER_t)} \right] \quad (11)$$

Equation 11 is of course identical to eq 10 (note that $(1 + ER_t) = C_t/A_2$) and thus gives the identical enrichment factor, $\varepsilon_2 = -(\bar{k}/k_2)$, and eq 12 is identical to eq 9 with an enrichment factor, $\varepsilon_1 = -(\bar{k}/k_1)$.

$$\ln \frac{ER_t}{ER_0} = \varepsilon_1 \times \ln \frac{C_t}{C_0} \left[\frac{(1 + 1/ER_0)}{(1 + 1/ER_t)} \right] \quad (12)$$

Figures S1 and S2 in the SI depict the graphical form of eqs 9 and 10 for each enzyme and microcosm study and the slopes of the linear curves and their 95% confidence interval are presented as the respective chiral enrichment factors in Table S1 in the SI.

Thus, the three forms of 'Rayleigh equation' are transformable. The enrichment factor of eqs 9 and 12, ε_1 , can be obtained from eq 8 by multiplication of ε_{ER} by k_c/k_1 and ε_2 can be obtained from ε_1 by multiplication of ε_1 by k_1/k_2 . The 'general' Rayleigh equation and its conventional form become identical when ER is very large giving the same slope of the \ln - \ln curve.

Table S1 in the SI depicts the individual linear kinetic coefficients (k_1, k_2 and k_c) of each of the species involved (A_1, A_2 , and C) and the enantiomeric (Rayleigh) enrichment factors based on these three different variables (ε_1 , ε_2 , and ε_{ER}). Columns 9, 10, 11, and 12 show that indeed the ratio between

the slopes of the Rayleigh equations is very close in all cases to the ratio between the respective experimentally derived rates coefficients. Moreover, the transformations from ε_1 to ε_2 (corresponding to transformations between different general Rayleigh forms) were not better predicted than the transformations between ε_{ER} and ε_1 .

In principle, the “general” Rayleigh equation is not limited to linear kinetics, but it includes all the cases in which the kinetics of formation of the two species A_1 and A_2 are connected by expression 13:

$$\frac{dA_1}{A_1} \propto \frac{dA_2}{A_2} \quad (13)$$

Which implies that the individual kinetics is described by the expressions of the following form (eqs 14,15):

$$\frac{dA_1}{dt} = -k_1 A_1 F_{(A_1, A_2)} \quad (14)$$

$$\frac{dA_2}{dt} = -k_2 A_2 F_{(A_1, A_2)} \quad (15)$$

Where $F_{(A_1, A_2)}$ is a common general function which is identical for the degradation or formation of the two enantiomers. When F is a unity function independent of A_1 and A_2 then both enantiomers degrade by first order rate law. Other cases are very uncommon and imply a complicated mode of activation (or inhibition) of the degradation of each of the enantiomers by only one of them. Thus, in practice when linear kinetics is not guaranteed, eq 13 is very unlikely to prevail as well, and then one should resort to the full selectivity expression instead of using the Rayleigh law.

A Condition for a Linear Observed Rate Law For C. The Michaelis–Menten rate law is rather widely used to fit enzymatic reaction rates, and requires no elucidation here. The law gives linear dependence when the concentration of the substrate C , is much lower than the saturation constant, K_M (eq 16).

$$C \ll K_M \quad (16)$$

In fact, most of the environmental pollutants are reported by comprehensive surveys and monitoring reviews to be at very low concentrations, which in most cases are at least 3 orders of magnitude lower than the Michaelis–Menten constants that are indicated in the literature for the various enzymes. The highest concentrations found in the environment are in the range of the smallest K_M values (Tables S4, S5 in the SI). Therefore, it is not surprising that most enzymatic processes in the environment will follow first order kinetics. Note that wastewater treatment systems are excluded from this discussion. Rayleigh conditions are seldom met there, since they involve some highly mixed biological reactors, which do not follow the Rayleigh law even for isotopes, for detailed explanation, see the SI.

Thus, the fact that linear degradation is rather abundant is hardly a surprise. However, eq 5 and its linear form are also widely used for the description of reactions of chiral pairs.⁴⁷ In fact only a very small percentage of the literature data on degradation of chiral compounds considers fractionation, so it seems that in most cases there is no practical need to discern the individual enantiomeric behavior, simply because the deviation from the Michaelis–Menten expression is mostly within the experimental error. However, strictly speaking, linear dependence of the pair of enantiomers, A_1 and A_2 where each one obeys linear kinetics does involve an approximation.

Consider again the pair of enantiomers A_1 , A_2 , and their sum C . From eq 5, the rate law for C is given by eq 17.

$$\begin{aligned} \frac{dC}{dt} &= -k_1 A_1 - k_2 A_2 \\ &= -k_2 (A_1 + A_2) - (k_1 - k_2) A_1 \\ &= -k_2 C + \bar{k} A_1 \end{aligned} \quad (17)$$

Thus, when $\bar{k} A_1$ is very small compared to $k_2 C$ (eq 18) a first rate expression is obtained. This is often the case when $k_1 \approx k_2$ or when $A_1 \ll A_2$ (as is the case for organic isotopomers).

$$k_2 \times C \gg \bar{k} \times A_1 \quad (18)$$

A similar derivation but with adding and subtracting $k_1 A_2$ to the linear rate law of eq 17 gives another condition (independent of eq 18) for overall observed linearity (eq 19).

$$k_1 \times C \gg \bar{k} \times A_2 \quad (19)$$

Interestingly, when $k_2 \gg k_1$ then after a short reaction progress the condition $A_2 \ll A_1$ is established and then the condition in eq 19 is guaranteed. So, in practice, in many cases a linear fit of the degradation is valid for most of the experimentally acquired data points.

Summing the arguments above, it seems that the Rayleigh equation can be safely employed when the enantiomer degradation follows a Michaelis–Menten degradation rate under two conditions: the concentration of the substrate is much lower than the saturation constant, K_M (eq 16), and linear overall degradation kinetic process is observed (by assuring the conditions in eqs 18 or 19). Exceptions can be found especially when the more labile enantiomer is originally present at much higher concentration than the other enantiomer.

In all our experimental cases the validity conditions developed above held true; the concentration of the studied analytes was much lower than the Michaelis–Menten saturation constants. Due to this, the results were consistently in the first order range of the Michaelis–Menten kinetics, giving a first order kinetic fit in all cases with a correlation coefficient in the range of 0.93–0.99 (detailed in SI, Table S1, column 8). Additionally, the rate law of the pair of enantiomers matched the linear rate law, thus assuring the condition of expression 19 in all cases as detailed in the SI Table S1 column 13. In the worst case (i.e., at the initial conditions when $A_1 = A_2$) the conditions result in the factor of 2.6, but if we disregard a single extreme point in the kinetic data, the range starts at the factor 15. In the microcosm case studies the worst case points of the Rayleigh fit are in the range of 2.1–9.5 and when disregarding the first data point, the minimal factor is 5.

ENVIRONMENTAL SIGNIFICANCE

In the present study we demonstrate a suitability of the Rayleigh equation for assessing the extent of degradation of chiral organic compounds and derived a set of kinetic conditions for the validity of the Rayleigh equation for chiral analysis. The option of modeling enantioselective processes by employing the Rayleigh equation allows the derivation of an enantiomeric enrichment factor (ε_{ER}), which can be used as a characteristic tool for a specific enzymatic reaction. Implementation of two-dimensional isotope-enantiomeric enrichment approach can be advantageous for distinguishing between biotic and abiotic degradation pathways. In cases, where the use of the

isotope analysis is limited or uninformative, it can be replaced by the enantiomeric approach.

■ ASSOCIATED CONTENT

● Supporting Information

Experimental details, a table detailing first order kinetic constants, Rayleigh constants and validity conditions of the Rayleigh approach for our enzymatic experiment and microcosm reported studies, two figures displaying the graphical form of eqs 9 and 10 for each enzyme and microcosm study, a table detailing the slopes of the 2-d plots, table of analogy and difference between isotope and enantiomeric enrichment, a table detailing reported K_M saturation constants in comparison to the typical environmental concentration ranges of pollutants and a detailed explanation regarding the inapplicability of the Rayleigh equation for continuously mixed flow reactors are available free of charge via the Internet at <http://pubs.acs.org>.

■ AUTHOR INFORMATION

Corresponding Authors

*(F.G.) Phone: +972 25 314 208; e-mail: faina@gsi.gov.il.

*(O.L.) Phone: +972(0)26584191; fax: +972(0)26586155; e-mail: ovadia@mail.huji.ac.il.

Author Contributions

This manuscript is part of the PhD thesis of S. Jammer under the guidance of O. Lev and F. Gelman. A. Voloshenko participated in guidance and instrumentation. All authors have given approval to the final version of the manuscript.

Notes

The authors declare no competing financial interest.

■ ACKNOWLEDGMENTS

We are grateful to the Israel Water Authority, the Israel—Germany Water Technology Program of the BMBF—Germany and MOS—Israel and TEVA Pharmaceutical Industries Ltd. for the financial support of this study.

■ REFERENCES

- (1) Elsner, M.; Jochmann, M. A.; Hofstetter, T. B.; Hunkeler, D.; Bernstein, A.; Schmidt, T. C.; Schimmelmann, A. Current challenges in compound-specific stable isotope analysis of environmental organic contaminants. *Anal. Bioanal. Chem.* **2012**, *403* (9), 2471–91.
- (2) Thullner, M.; Centler, F.; Richnow, H.-H.; Fischer, A. Quantification of organic pollutant degradation in contaminated aquifers using compound specific stable isotope analysis – Review of recent developments. *Org. Geochem.* **2012**, *42* (12), 1440–1460.
- (3) Elsner, M. Stable isotope fractionation to investigate natural transformation mechanisms of organic contaminants: Principles, prospects and limitations. *J. Environ. Monit.* **2010**, *12* (11), 2005–31.
- (4) Meyer, A. H.; Penning, H.; Elsner, M. C and N isotope fractionation suggests similar mechanisms of microbial atrazine transformation despite involvement of different enzymes (AtzA and TrzN). *Environ. Sci. Technol.* **2009**, *43* (21), 8079–85.
- (5) Hartenbach, A. E.; Hofstetter, T. B.; Tentscher, P. R.; Canonica, S.; Berg, M.; Schwarzenbach, R. P. Carbon, hydrogen, and nitrogen isotope fractionation during light-induced transformations of atrazine. *Environ. Sci. Technol.* **2008**, *42* (21), 7751–6.
- (6) Penning, H.; Sorensen, S. R.; Meyer, A. H.; Aamand, J.; Elsner, M. C, N, and H isotope fractionation of the herbicide isoproturon reflects different microbial transformation pathways. *Environ. Sci. Technol.* **2010**, *44* (7), 2372–8.
- (7) Wiegert, C.; Aeppli, C.; Knowles, T.; Holmstrand, H.; Evershed, R.; Pancost, R. D.; Machackova, J.; Gustafsson, O. Dual carbon-chlorine stable isotope investigation of sources and fate of chlorinated

ethenes in contaminated groundwater. *Environ. Sci. Technol.* **2012**, *46* (20), 10918–25.

(8) Reinnicke, S.; Simonsen, A.; Sorensen, S. R.; Aamand, J.; Elsner, M. C and N isotope fractionation during biodegradation of the pesticide metabolite 2,6-dichlorobenzamide (BAM): Potential for environmental assessments. *Environ. Sci. Technol.* **2012**, *46* (3), 1447–54.

(9) Fischer, A.; Herklotz, I.; Herrmann, S.; Thullner, M.; Weelink, S. A.; Stams, A. J.; Schlomann, M.; Richnow, H. H.; Vogt, C. Combined carbon and hydrogen isotope fractionation investigations for elucidating benzene biodegradation pathways. *Environ. Sci. Technol.* **2008**, *42* (12), 4356–63.

(10) Vogt, C.; Cyrus, E.; Herklotz, I.; Schlosser, D.; Bahr, A.; Herrmann, S.; Richnow, H. H.; Fischer, A. Evaluation of toluene degradation pathways by two-dimensional stable isotope fractionation. *Environ. Sci. Technol.* **2008**, *42* (21), 7793–800.

(11) Herrmann, S.; Vogt, C.; Fischer, A.; Kuppardt, A.; Richnow, H. H. Characterization of anaerobic xylene biodegradation by two-dimensional isotope fractionation analysis. *Environ. Microbiol. Rep.* **2009**, *1* (6), 535–44.

(12) Rosell, M.; Finsterbusch, S.; Jechalke, S.; Hubschmann, T.; Vogt, C.; Richnow, H. H. Evaluation of the effects of low oxygen concentration on stable isotope fractionation during aerobic MTBE biodegradation. *Environ. Sci. Technol.* **2010**, *44* (1), 309–15.

(13) Youngster, L. K.; Rosell, M.; Richnow, H. H.; Haggblom, M. M. Assessment of MTBE biodegradation pathways by two-dimensional isotope analysis in mixed bacterial consortia under different redox conditions. *Appl. Microbiol. Biotechnol.* **2010**, *88* (1), 309–17.

(14) Jechalke, S.; Rosell, M.; Martinez-Lavanchy, P. M.; Perez-Leiva, P.; Rohwerder, T.; Vogt, C.; Richnow, H. H. Linking low-level stable isotope fractionation to expression of the cytochrome P450 monooxygenase-encoding ethB gene for elucidation of methyl tert-butyl ether biodegradation in aerated treatment pond systems. *Appl. Environ. Microbiol.* **2011**, *77* (3), 1086–96.

(15) Morrill, P. L.; Sleep, B. E.; Slater, G. F.; Edwards, E. A.; Lollar, B. S. Evaluation of isotopic enrichment factors for the biodegradation of chlorinated ethenes using a parameter estimation model: Toward an improved quantification of biodegradation. *Environ. Sci. Technol.* **2006**, *40* (12), 3886–92.

(16) Abe, Y.; Aravena, R.; Zopf, J.; Shouakar-Stash, O.; Cox, E.; Roberts, J. D.; Hunkeler, D. Carbon and chlorine isotope fractionation during aerobic oxidation and reductive dechlorination of vinyl chloride and cis-1,2-dichloroethene. *Environ. Sci. Technol.* **2009**, *43* (1), 101–7.

(17) Zwank, L.; Berg, M.; Elsner, M.; Schmidt, T. C.; Schwarzenbach, R. P.; Haderlein, S. B. New evaluation scheme for two-dimensional isotope analysis to decipher biodegradation processes: Application to groundwater contamination by MTBE. *Environ. Sci. Technol.* **2005**, *39* (4), 1018–29.

(18) Fischer, A.; Theuerkorn, K.; Stelzer, N.; Gehre, M.; Thullner, M.; Richnow, H. H. Applicability of stable isotope fractionation analysis for the characterization of benzene biodegradation in a BTEX-contaminated aquifer. *Environ. Sci. Technol.* **2007**, *41* (10), 3689–96.

(19) Bernstein, A.; Adar, E.; Ronen, Z.; Lowag, H.; Stichler, W.; Meckenstock, R. U. Quantifying RDX biodegradation in groundwater using delta-15N isotope analysis. *J. Contam. Hydrol.* **2010**, *111* (1–4), 25–35.

(20) MacLeod, S. L.; Wong, C. S. Loadings, trends, comparisons, and fate of achiral and chiral pharmaceuticals in wastewaters from urban tertiary and rural aerated lagoon treatments. *Water Res.* **2010**, *44* (2), 533–44.

(21) Barreiro, J. C.; Vanzolini, K. L.; Madureira, T. V.; Tiritan, M. E.; Cass, Q. B. A column-switching method for quantification of the enantiomers of omeprazole in native matrices of waste and estuarine water samples. *Talanta* **2010**, *82* (1), 384–91.

(22) MacLeod, S. L.; Sudhir, P.; Wong, C. S. Stereoisomer analysis of wastewater-derived beta-blockers, selective serotonin re-uptake inhibitors, and salbutamol by high-performance liquid chromatography-tandem mass spectrometry. *J. Chromatogr. A* **2007**, *1170* (1–2), 23–33.

- (23) Wong, C. S. Environmental fate processes and biochemical transformations of chiral emerging organic pollutants. *Anal. Bioanal. Chem.* **2006**, *386* (3), 544–58.
- (24) Fono, L. J.; Sedlak, D. L. Use of the chiral pharmaceutical propranolol to identify sewage discharges into surface waters. *Environ. Sci. Technol.* **2005**, *39* (23), 9244–52.
- (25) Matamoros, V.; Hijosa, M.; Bayona, J. M. Assessment of the pharmaceutical active compounds removal in wastewater treatment systems at enantiomeric level. Ibuprofen and naproxen. *Chemosphere* **2009**, *75* (2), 200–205.
- (26) Hijosa-Valsero, M.; Matamoros, V.; Martin-Villacorta, J.; Becares, E.; Bayona, J. M. Assessment of full-scale natural systems for the removal of PPCPs from wastewater in small communities. *Water Res.* **2010**, *44* (5), 1429–39.
- (27) Zipper, C.; Suter, M. J.; Haderlein, S. B.; M., G.; Kohler, H. E. Changes in the enantiomeric ratio of (R)- to (S)-mecoprop indicate in situ biodegradation of this chiral herbicide in a polluted aquifer. *Environ. Sci. Technol.* **1998**, *32* (14), 2070–2076.
- (28) Monkiedje, A.; Spiteller, M.; Bester, K. Degradation of racemic and enantiopure metalaxyl in tropical and temperate soils. *Environ. Sci. Technol.* **2003**, *37* (4), 707–12.
- (29) Jaeger, K. E.; Ransac, S.; Dijkstra, B. W.; Colson, C.; van Heuvel, M.; Misset, O. Bacterial lipases. *FEMS Microbiol. Rev.* **1994**, *15* (1), 29–63.
- (30) Sonnet, P. E.; Gazzillo, J. A. Evaluation of lipase selectivity for hydrolysis. *J. Am. Oil Chem. Soc.* **1991**, *68* (1), 11–15.
- (31) Strohalm, H.; Dold, S.; Pendzialek, K.; Weiher, M.; Engel, K. H. Preparation of passion fruit-typical 2-alkyl ester enantiomers via lipase-catalyzed kinetic resolution. *J. Agric. Food Chem.* **2010**, *58* (10), 6328–33.
- (32) Monroy-Noyola, A.; Sogorb, M. A.; Vilanova, E. Enzyme Concentration as an Important Factor in the In Vitro Testing of the Stereospecificity of the Enzymatic Hydrolysis of Organophosphorus Compounds. *Toxicol. In Vitro* **1999**, *13* (4–5), 689–692.
- (33) Marten, E.; Muller, R. J.; Deckwer, W. D. Studies on the enzymatic hydrolysis of polyesters: I. Low molecular mass model esters and aliphatic polyesters. *Polym. Degrad. Stab.* **2003**, *80*, 458–501.
- (34) Badea, S. L.; Vogt, C.; Gehre, M.; Fischer, A.; Danet, A. F.; Richnow, H. H. Development of an enantiomer-specific stable carbon isotope analysis (ESIA) method for assessing the fate of alpha-hexachlorocyclo-hexane in the environment. *Rapid Communications in Mass Spectrometry* **2011**, *25* (10), 1363–72.
- (35) Maier, M. P.; Qiu, S.; Elsner, M. Enantioselective stable isotope analysis (ESIA) of polar herbicides. *Anal. Bioanal. Chem.* **2013**, *405* (9), 2825–31.
- (36) Gasser, G.; Pankratov, I.; Elhanany, S.; Werner, P.; Gun, J.; Gelman, F.; Lev, O. Field and laboratory studies of the fate and enantiomeric enrichment of venlafaxine and O-desmethylvenlafaxine under aerobic and anaerobic conditions. *Chemosphere* **2012**, *88* (1), 98–105.
- (37) Zipper, C.; Bunk, M.; Zehnder, A. J.; Kohler, H. P. Enantioselective uptake and degradation of the chiral herbicide dichlorprop [(RS)-2-(2,4-dichlorophenoxy)propanoic acid] by *Sphingomonas herbicidovorans* MH. *J. Bacteriol.* **1998**, *180* (13), 3368–74.
- (38) Ma, Y.; Xu, C.; Wen, Y.; Liu, W. Enantioselective separation and degradation of the herbicide dichlorprop methyl in sediment. *Chirality* **2009**, *21* (4), 480–3.
- (39) Diao, J.; Xu, P.; Wang, P.; Lu, D.; Lu, Y.; Zhou, Z. Enantioselective degradation in sediment and aquatic toxicity to *Daphnia magna* of the herbicide lactofen enantiomers. *J. Agric. Food Chem.* **2010**, *58* (4), 2439–45.
- (40) Zhang, Y.; Liu, D.; Diao, J.; He, Z.; Zhou, Z.; Wang, P.; Li, X. Enantioselective environmental behavior of the chiral herbicide fenoxaprop-ethyl and its chiral metabolite fenoxaprop in soil. *J. Agric. Food Chem.* **2010**, *58* (24), 12878–84.
- (41) Amirav, A. Electron impact and hyperthermal surface ionization mass spectrometry in supersonic molecular beams. *Org. Mass Spectrom.* **1991**, *26* (1), 1–17.
- (42) Aelion, C. M.; Höhener, P.; Hunkeler, D.; Aravena, R. *Environ. Isotopes in Biodegradation and Bioremediation*; CRC Press, 2010; p 69–71.
- (43) Smith, M. B.; March, J. *Organic Chemistry, Reactions, Mechanisms and Structure*, 6th ed.; John Wiley & sons, Inc, 2007.
- (44) Bergmann, F. D.; Abu Laban, N. M.; Meyer, A. H.; Elsner, M.; Meckenstock, R. U. Dual (C, H) isotope fractionation in anaerobic low molecular weight (poly)aromatic hydrocarbon (PAH) degradation: Potential for field studies and mechanistic implications. *Environ. Sci. Technol.* **2011**, *45* (16), 6947–53.
- (45) Rayleigh, J. W. S. Theoretical considerations respecting the separation of gases by diffusion and similar processes. *Philos. Mag.* **1896**, *42*, 493–498.
- (46) Bashir, S.; Fischer, A.; Nijenhuis, I.; Richnow, H. H. Enantioselective carbon stable isotope fractionation of hexachlorocyclohexane during aerobic biodegradation by *Sphingobium* spp. *Environ. Sci. Technol.* **2013**, *47* (20), 11432–9.
- (47) Dixon, M.; Webb, M.; Edwin, C. *Enzymes*, Bernard Axelrod. *J. Chem. Educ.* **1965**, *42*, 486–488.
- (48) Huhnerfuss, H.; Shah, M. R. Enantioselective chromatography—a powerful tool for the discrimination of biotic and abiotic transformation processes of chiral environmental pollutants. *J. Chromatogr. A* **2009**, *1216* (3), 481–502.